Novel ARC Optimization Methodology for KrF Excimer Laser Lithography at Low K1 Factor

H01L 21/027 B64
G03F 7/09 A

Tohru Ogawa, Mitsunori Kimura, Yoichi Tomo,
and Toshiro Tsumori

XP-002130896

Process Technology Division, ULSI R&D Group, SONY Corporation
(4-14-1 Asahi-cho, Atsugi-shi, Kanagawa-ken, 243 Japan)

11-03-'92
362.375 14

ABSTRACT

This paper describes a new anti-reflective coating (ARC) optimization methodology, and reports a practical new ARC material and its actual performance for KrF excimer laser lithography as an application of this methodology.

First, the optimal optical conditions, refractive index and thickness, for ARC are defined as those values that cause the minimal energy absorption fluctuation for various in a photoresist thicknesses. To find optimal optical conditions, we calculated the energy absorbed in a photoresist for continuously different ARC optical conditions using a multi thin-film interference simulator based on the matrix method for various photoresist thicknesses. As an application results of this method, we show optimal ARC optical conditions, i.e. refractive indices for various thicknesses, for a tungsten silicide (W-Si) substrate, which is highly reflective and the critical layer for KrF excimer laser lithography.

Next, we searched for a practical material to be used as an ARC whose refractive indices were closest to the optimal conditions. From these results, we found a novel and practical material for optical lithography. Silicon carbide (SiC) films satisfied optimal optical conditions as an ARC for W-Si substrates. For the swing ratio, a photoresist absorption variation of ±21% without SiC was reduced to less than ±1% with SiC.

Finally, in order to achieve an ARC performance on actual structures, we optimized the SiC refractive index as an ARC for W-Si substrates using various ECR Plasma CVD conditions. As a result, we obtained a high performance ARC for W-Si substrates. A critical dimension variation of 0.12μm without SiC was reduced to less than 0.02μm with SiC for 0.35um L/S.

1. Introduction

Thin-film interference effects in photoresists are well known phenomena when using monochromatic illumination exposure tools, e.g. stepper systems[1,2]. This effect changes the fraction of the energy available for photoresist absorption and subsequently causes serious line-width fluctuation[3]. Thus, accurate line-width control requires the reduction of this effect. In the current status of KrF excimer laser lithography, this effect is the most serious issue with highly transparent photoresists, which yield the highest resolution and most vertical profiles, because the refractive index of the substrate in deep UV region is larger than that for g- or i-line lithography, and as a result, as many paper have already reported, reflections from the substrate are strong. Anti-reflective techniques using an inorganic or organic thin film are well known processes to reduce thin-film interference effects in photoresists. Although many organic ARC have already been reported[4,5,6,7], a high performance and theoretically optimized inorganic ARC which is suitable for low K1 factor in Rayleigh criteria has not been reported. Therefore, for excimer laser lithography to become a practical tool for device production, a high performance ARC should be developed.

BEST AVAILABLE COPY

2. ARC Optimization

In this section, we describe the theoretical method for high performance inorganic ARC optimization. In particular, we investigate on ARC's ideal optical conditions which minimize the energy absorption fluctuation in photoresist for photoresist thickness variation using a simulator for a multilayer thin-film.

2.1. Simulator for a multilayer thin-film

A computer program has been developed to calculate reflectance, transmittance, and absorption of a multilayer thin-film. Figure 1 shows a schematic view of a multilayer thin-film. In this figure, there are m layered materials where the 0-th layer is assumed to be air and the m-th layer to be a substrate. Lj is the thickness of the j-th layer and Nj is the complex refractive index of which the real part is nj and the imaginary part is -kj, i.e. Nj = nj - ikj. The program calculates reflectance, transmittance, and absorption when light of wavelength λ enters the multilayer thin-film with incident angle $\Phi 0$.

According to Maxwell's equations, at the boundary of different materials, the electric and magnetic field normal to the boundary surface are continuous. So, the electric field Ej normal to the interface between the j-th and (j+1)-th layer can be defined. In the same way, the magnetic field Hj normal to the j-th interface is also defined. These fields Ej, Hj satisfy equation (1)[8].

$$\begin{bmatrix} E_{j-1} \\ H_{j-1} \end{bmatrix} = \begin{bmatrix} \cos\Phi_j & (i/\overline{N_j})\sin\Phi_j \\ i\overline{N_j}\sin\Phi_j & \cos\Phi_j \end{bmatrix} \begin{bmatrix} E_j \\ H_j \end{bmatrix} \quad \cdots (1)$$

$\overline{N_j}$ and Φj in this equation are defined respectively as follows:

$$\overline{N_j} \equiv \frac{N_j}{\cos\Phi_j} \text{ (p-polarization)}$$

$$\text{or } N_j\cos\Phi_j \text{ (s-polarization)} \quad , \text{and} \quad \Phi_j \equiv \frac{2\pi}{\lambda} N_j L_j \cos\Phi_j$$

And Φj is evaluated using:

$$N_j \sin\Phi_j = n_0 \sin\Phi_0$$

In the m-th layer, there are only transmitting waves, consequently,

$$\begin{aligned} E_{m-1} &= 1 \\ H_{m-1} &= \overline{N_m} \end{aligned} \quad \cdots (2)$$

Using equations (1) and (2), the fields Ej, and Hj are determined from the (m-1)-th interface to the 0-th interface. Once the fields at each interface are determined, the reflectance R, transmittance T and absorption of the j-th layer Aj are calculated using the following equation.

$$R = \left| \frac{E_0 - (H_0 / \overline{n_0})}{E_0 + (H_0 / \overline{n_0})} \right|$$

$$T = \frac{4\,\mathrm{Re}[\overline{N_m}]}{|\overline{n_0}|\,|E_0 + (H_0/\overline{n_0})|^2}$$

$$A_j = \frac{\mathrm{Re}\left[E_{j-1}H_{j-1}^*\right] - \mathrm{Re}\left[E_jH_j^*\right]}{(\overline{n_0}/4)\,|E_0 + (H_0/\overline{n_0})|^2}$$

Figure 2 shows a comparison between calculated resist absorption and remaining photoresist thickness after exposure, i.e. experimental results. Matching condition are shown in Table 1. For the matching test, the indices of refraction at 248nm for XP8843 photoresist (n=1.802, k=0.011), and a bare silicon substrate (n=1.572, k=3.583) were measured using a spectroscopic ellipsometer. The remaining photoresist thickness after exposured with constant dose for various photoresist thicknesses varies due to thin-films interference effects. When energy absorption in XP8843 photoresists are high, the remaining photoresist thickness after exposure are thick, because XP8843 is a negative photoresist. As shown in Figure 2, calculations and experiments shows good agreement.

2.2. Design specification for ARC

To obtain a quantitative specification for high performance ARC optimization in KrF excimer laser lithography, critical dimension variations caused by photoresist absorption fluctuations were investigated.

Figure 3 shows calculated photoresist thickness versus normalized photoresist absorption and measured critical dimensions for nominal (a) 0.50μm L/S, (b) 0.40μm L/S, and (c) 0.35μm L/S. The exposure tool for imaging was a Nikon KrF excimer laser stepper NSR-1505EX1 (λ:248nm, NA:0.42, 21.2mm diameter lens) equipped with a Cymer CX-2LS laser. The photoresist used was Shipley XP8843 chemically amplified negative photoresist, coated on a Silicon substrate. Both dense and window patterns were imaged on various photoresist thicknesses, and maesurements were then performed by a SEM at best focus. As shown in this figure, when the K1 factor in Rayleigh criteria decreases, thin-film interference effects in photoresists occur more readily and critical dimension variation increases. Accordingly, in the design of an ARC, the target K1 factor must be taken into consideration.

Figure 4 shows normalized critical dimension versus normalized photoresist absorption for nominal 0.50μm L/S, 0.40μm L/S, and 0.35μm L/S patterns. This figure is obtained from analyzing Figure 3. The figure suggest that, if critical dimension control is required to be within ±5% for a nominal line-width, photoresist absorption tolerances are required to be within ±6.5%, ±4%, ±3%, for 0.847, 0.677, 0.593 K1 factors respectively, as shown in Table 2. Moreover, notching phenomena due to halation [9] from various step heights and sidewalls or substrate films thickness variations are serious issues in actual device fabrication.

In the research and development of 0.35μm rule devices, even if a KrF excimer laser stepper is used as lithography tool, which has 0.37 to 0.45 NA, the K1 factor is as low as 0.52 to 0.64. In device fabrication under the constraint of a low K1 factor, a high performance ARC corresponding to such low K1 factors are required.

From the above discussion, in the current status, maximum photoresist absorption tolerances are required to be less than ±3% for high accuracy line-width control at low K1 factors and an ARC is required to satisfy this tolerance level.

2.3. Inorganic ARC design concept

Without an ARC, thin-film interference effects in photoresists are dependent upon each layer's refractive index at exposure wavelength λ. The value of the refractive index is fixed when a specific material and device structure is defined. On the other hand, as shown in Figure 5, when an ARC is placed between the photoresist and the substrate, thin-film interference effects in the photoresist are affected by the refractive index and thickness of the ARC. The optimal optical conditions for the ARC, refractive index n (real part), k

BEST AVAILABLE COPY

(imaginary part), and thickness d, are defined as those values that cause the minimal energy absorption fluctuation for a variation in photoresist thickness.

To find the optimal optical condition as an ARC, the following new methodology was adopted.

1. For a given photoresist and ARC thickness, calculate the energy absorption in the photoresist as a function of the continuously varying values of the complex refractive index of the ARC.
2. Change the values of the photoresist thickness and perform part 1 again.
3. Compare plots of equi-energy-absorption contours for the various photoresist thicknesses, and obtain common regions or closest points where the difference in energy absorptions are low.
4. Carry out parts 1 to 3 for other ARC thicknesses.
5. Determine the optimal refractive indices n and k for various ARC thicknesses d.

This methodology gives one direction for optimizing an ARC for some target substrate. Using this method, for any given substrate and ARC thickness, the optimal optical conditions can be determined. Moreover, even if the exposure wavelength is changed, the methodology does not change. In this case, the values of refractive indices of the photoresist, substrate, and various films need only be determined and the simulations once again performed with these new parameters. Therefore, this concept is novel methodology for ARC optimization.

As an application of this method, an inorganic ARC for tungsten silicide (W-Si) substrates was optimized. Imaging on W-Si substrates is especially difficult due to it's high reflectivity when using a KrF excimer laser stepper. Additionally, high resolution patterning is usually required on these substrates. For this simulation, the refractive indices of the W-Si substrate and XP8843 chemically amplified photoresists at 248nm were measured by a spectroscopic ellipsometer and found to be n=1.96, k=2.69 and n=1.802, k=0.011 respectively.

Figure 6 shows some calculations of equi-energy absorption contours for four different photoresist thicknesses. The values of absorption are indicated near each equi-energy contour. In the simulation study performed, two common regions, indicated by the open circles in these figures, indicate the optimal points for a 30nm thick ARC. The refractive indices of these two regions are n=2.15, k=0.67 and n=4.90, k=0.10.

Figure 7 shows simulated thin-film interference effects in XP8843 photoresists both with (Figure 7b and 7c) and without an ARC (Figure 7a) for the two refractive indices shown above using a 30nm thick ARC. A photoresist absorption variation of ±21% in swing ratio without an ARC was reduced to less than ±2% using an ARC with a refractive index of n=2.15, k=0.67 (Figure 7b) and less than ±1.5% using an ARC with a refractive index of n=4.90, k=0.10 (Figure 7c).

Figure 8 shows the optimal ARC optical constants n and k for various ARC thicknesses d. Materials that satisfy the optimal optical constant curves indicated in this figure are appropriate as a high performance ARC for a W-Si substrate.

2.4. Material survey

To find a practical material whose refractive indices were closest to either of the optimal optical conditions shown in Figure 8, the refractive indices of various thin-films were

measured using a spectroscopic ellipsometer and subsequently searched for in the available literature[10].

Figure 9 shows measurements and checking results for refractive indices at 248nm. A new and practical material for optical lithography was able to be found from Figure 8 and Figure 9. The refractive index of Silicon Carbide (SiC) was listed as being n=3.17, k=0.22 in the literature. This value with a 50nm thickness satisfied condition (2) in Figure 8 completely. Therefore, a 50nm thick SiC film matched the optimal optical condition as an ARC for W-Si substrates.

Figure 10 shows the performance of the SiC film as an ARC for W-Si substrates as determined by simulation. Without the SiC film, the value of energy absorption fluctuated by ±21%. On the other hand, using a 50nm thick SiC film, thin-film interference effects are reduced to only ±1%. Therefore, SiC films is advantageous material as a high performance ARC for W-Si substrates.

3. Evaluation of actual SiC film

In this section, we describe optimization results for refractive indices of actual SiC film as an ARC. Then we report the evaluation results for an optimized SiC film for W-Si substrates using a KrF excimer laser stepper Nikon NSR-1505EX1 (NA=0.42, 21.2mm diameter lens) equipped with a cymer CX-2LS laser and Shipley XP8843 chemically amplified photoresist.

3.1. Optical characteristics

In order to achieve the results shown in section 2.4, SiC films were deposited with various ECR Plasma CVD conditions. Subsequently, the refractive indices of the various SiC films were measured using a spectroscopic ellipsometer.

Figure 11 shows the refractive indices for the various deposition conditions. The refractive indices of the SiC films were strongly affected by the mole ratio in the source gas and weakly affected by the microwave power and gas pressure. Increasing the mole ratio of SiH_4, the refractive indices changes from 1.6 to 2.65 (real part) and from 0.25 to 1.6 (imaginary part).

The optimal optical condition for the actual SiC was determined both by utilizing the above results and a refractive index of n=1.93, k=2.73 for W-Si differed slightly that shown in section 2.3, and by utilizing a simulator for multilayer thin-films. Consequently, these values, real part n=2.36, imaginary part k=0.53, and thickness d=23.8nm, were adopted as a practical optimal ARC condition for W-Si substrates. Figure 12 shows the spectroscopic characterization of this ARC's refractive indices.

3.2. ARC performance

Figure 13 shows calculated photoresist absorption both with and without the practical SiC film. In this figure, the photoresist absorption fluctuation of ±21% without the SiC film was reduced to less than ±1.8% with the SiC film.

Figure 14 shows the optimized SiC film performance as an ARC for a flat W-Si substrate. This figure shows the photoresist thickness versus critical dimension for nominal (a) 0.50μm L/S, (b) 0.45μm L/S, (c) 0.40μm L/S, and (d) 0.35μm L/S. In this figure, both dense and window patterns are indicated by the circles, however the solid black circles indicate how the critical dimension varies without the SiC film and the open circles indicate the critical

BEST AVAILABLE COPY

dimension with the SiC film. With the SiC film, even for 0.35μm feature sizes, the critical dimension variation was reduced to within 0.02μm, as shown in Table 3.

Figure 15 shows the optimized SiC film performance as an ARC for W-Si substrates with a 35nm step. This step height is half period of the swing curve. This figure shows top view SEM photographs for nominal dense pattern 0.50μm L/S, 0.45μm L/S, 0.40μm L/S, and 0.35μm L/S both with and without SiC films. With SiC films, these patterns were acceptably resolved without notching phenomena or scum. Even for 0.35μm features, as shown in Table 3, the critical dimension variation over steps was reduced to within 0.035μm. This results in a ±5 % geometry control.

These results indicate that accurate line-width control can be achieved with a SiC film as an ARC for W-Si substrates. Additionally, these results proved that the methodology shown here to be useful for practical applications.

4. Conclusions

To control thin-film interference effects in photoresists effectively, we developed a novel optimization methodology for a high performance ARC. As an application of the methodology, we showed ideal ARC optical conditions for W-Si substrates using KrF excimer laser lithography. We found that a SiC film will be a novel and practical material for optical lithography. With SiC films, even if highly transparent photoresists were used for fine geometry imaging on W-Si substrates with a K1 factor less than 0.6, thin-film interference effects in photoresists are drastically reduced. This methodology also can be applied for other critical and highly reflective layers requiring high resolution patterning at low K1 factors. Therefore, we confirmed that by controlling thin-film interference effects in photoresists with the methodology shown here for ARC optimization, KrF excimer laser lithography will become a practical lithography tool for device production.

5. Acknowledgements

The authors would like to express their thanks to Takashi Shimada, Junichi Satoh, and Mikio Mukai for their beneficial advice and constant encouragement. The authors also would like thanks to Tetsuo Gotyou, Hideaki Hayakawa, and Masakazu Muroyama for their helpful advice on CVD growth.

6. References

1. D.D.Dunn, J.A.Bruce, M.S.Hibbs, "DUV photolithography linewidth variation from reflective substrates", Optical/Laser Microlithography IV., SPIE vol.1463, pp8-15, (1991).
2. B.Kuyel, H.Sewell, "The effect of broadband 250nm illumination on process latitude", J.Vac.Sci.Technol., vol.B8(6 pp1385-1391, (1990).
3. T.Ohfuji, M.Soenosawa, A.Nozue, K.Kasama, "Simulation Analysis of Deep-UV Chemically Amplified Resist", Optical/Laser Microlithography IV., SPIE vol.1463, pp345-354,(1991).
4. T.Tanaka, N.Hasegawa, H.Shiraishi, S.Okazaki, ""ARCOR", a new photolithography technique with antireflective coating on resist", Proceeding of Technical Conference on Photopolymers, pp195-203, (1991).
5. G.A.Barnes, S.K.Jones, B.W.Dudley, D.A.Koester, C.R.Peters, S.M.Bobbio, T.D.Flaim, "Anti-Reflective Coating for Deep UV Lithography Process Enhancement", Proceeding of Technical Conference on Photopolymers, pp259-270, (1991)

6. T.A.Brunner, "Optimization of optical properties of resist process", Advances in Resist Technology and Processing VIII., SPIE vol.1466, pp297-308.(1991).
7. S.Sethi, R.Distasio, D.Ziger, "Use of anti-reflective coatings in deep UV lithography", Optical/Laser Microlithography IV., SPIE vol.1463, pp30-40.(1991).
8. P.H.Berning, "Theory and Calculation of Optical Thin Films", Physics of thin film, vol.1, pp69-121, Academic Press, (1963).
9. M.W.Horn, "Antireflection Layers and Planarization for Microlithography", Solid State Technol, November, pp57-62, (1991).
10. E.D.Palik, Handbook of Optical Constants of Solids, Academic Press, Washington.D.C, (1985).

BEST AVAILABLE COPY

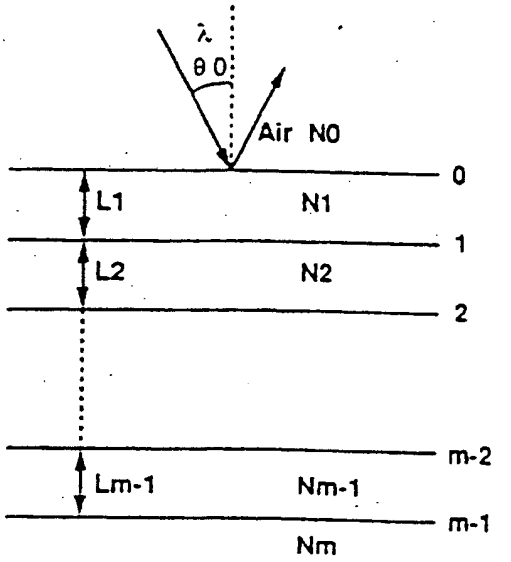

Figure 1. Schematic view of multilayer thin-film.

Table 1. Matching Condition

Resist	: XP8843, n=1.802, k=0.011
Substrate	: Bare Si, n=1.572, k=3.583
Exposure	: KrF excimer laser stepper NSR-1505EX1, λ = 248nm, NA 0.42
Dose	: 10mj/cm^2

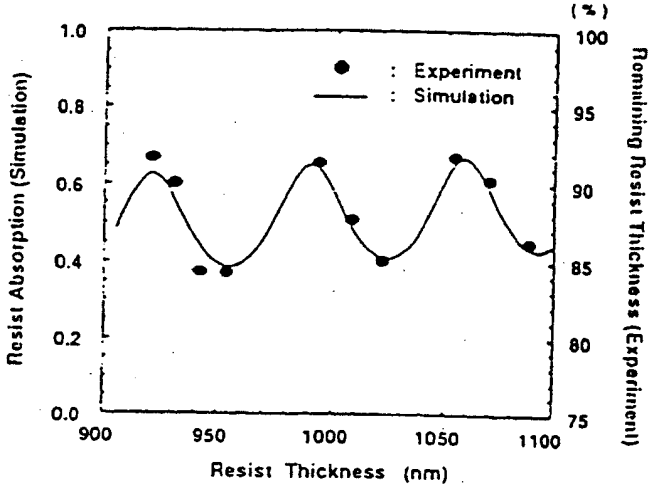

Figure 2. Resist thickness versus resist absorption (calculation) and remaining resist thickness after exposure(experiment).

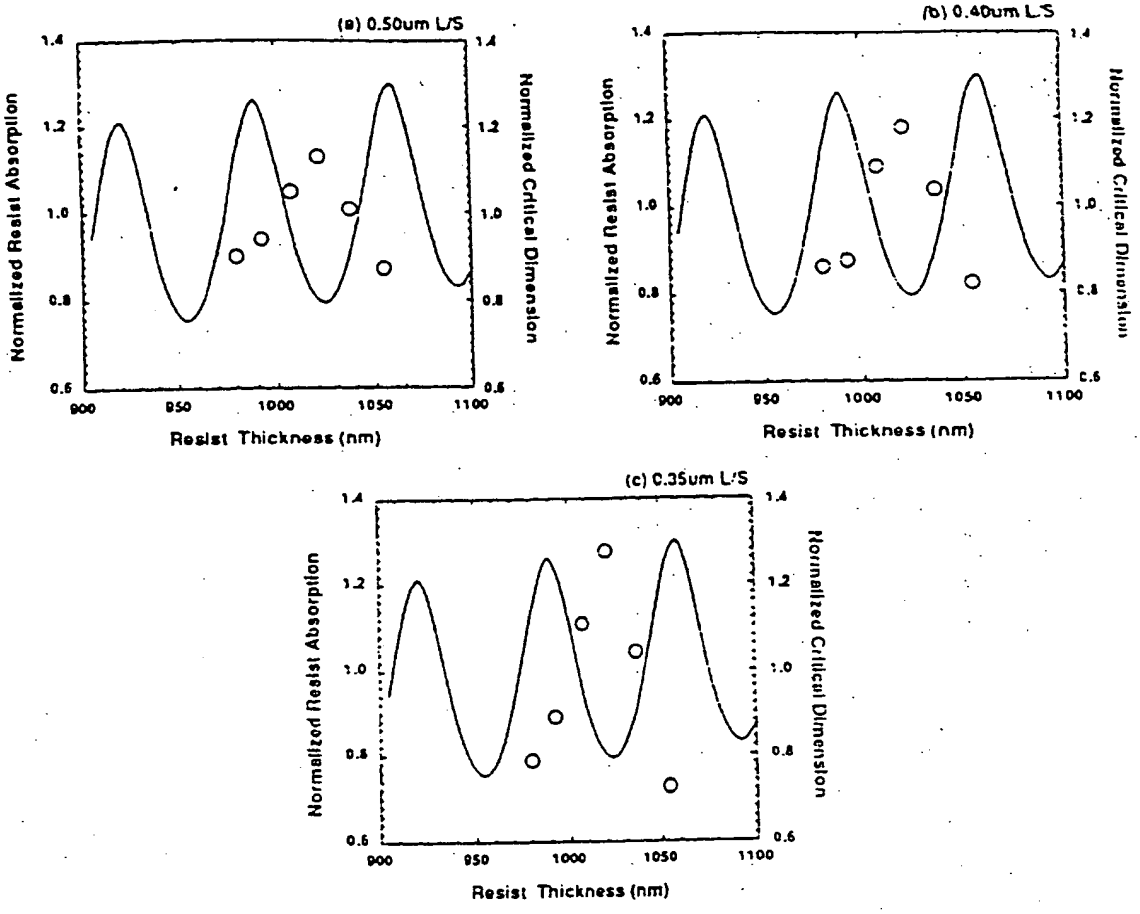

Figure 3. Simulation results of resist thickness versus normalized resist absorption (solid-line) and measured normalized critical dimension (open circles) for 0.50umL/S(a), 0.40umL/S(b), and 0.35umL/S(c).

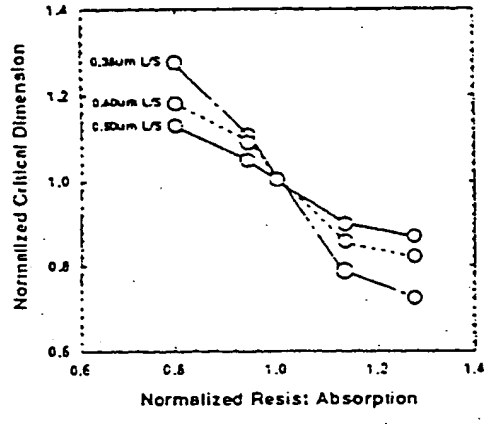

Figure 4. Normalized critical dimension versus normalized resist absorption for 0.50um L/S, 0.40um L/S, and 0.35um L/S.

Table 2. Tolerance of variation in resist absorption

Pattern Size	0.50um L/S	0.40um L/S	0.35um L/S
K1 Value	0.847	0.677	0.593
CD Specification (%)	± 5.0	± 5.0	± 5.0
Resist Absorption Tolerance (%)	± 6.5	± 4	± 3

BEST AVAILABLE COPY

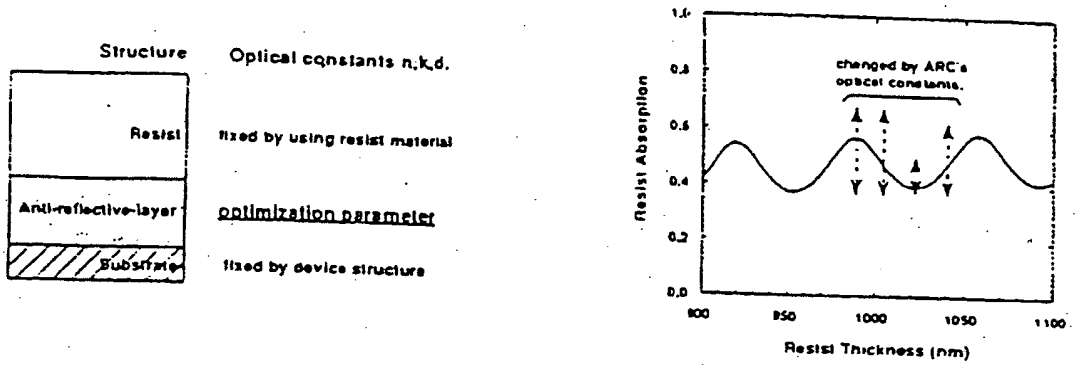

Figure 5. Schematic illustration of thin-film interference caused by ARC's optical conditions.

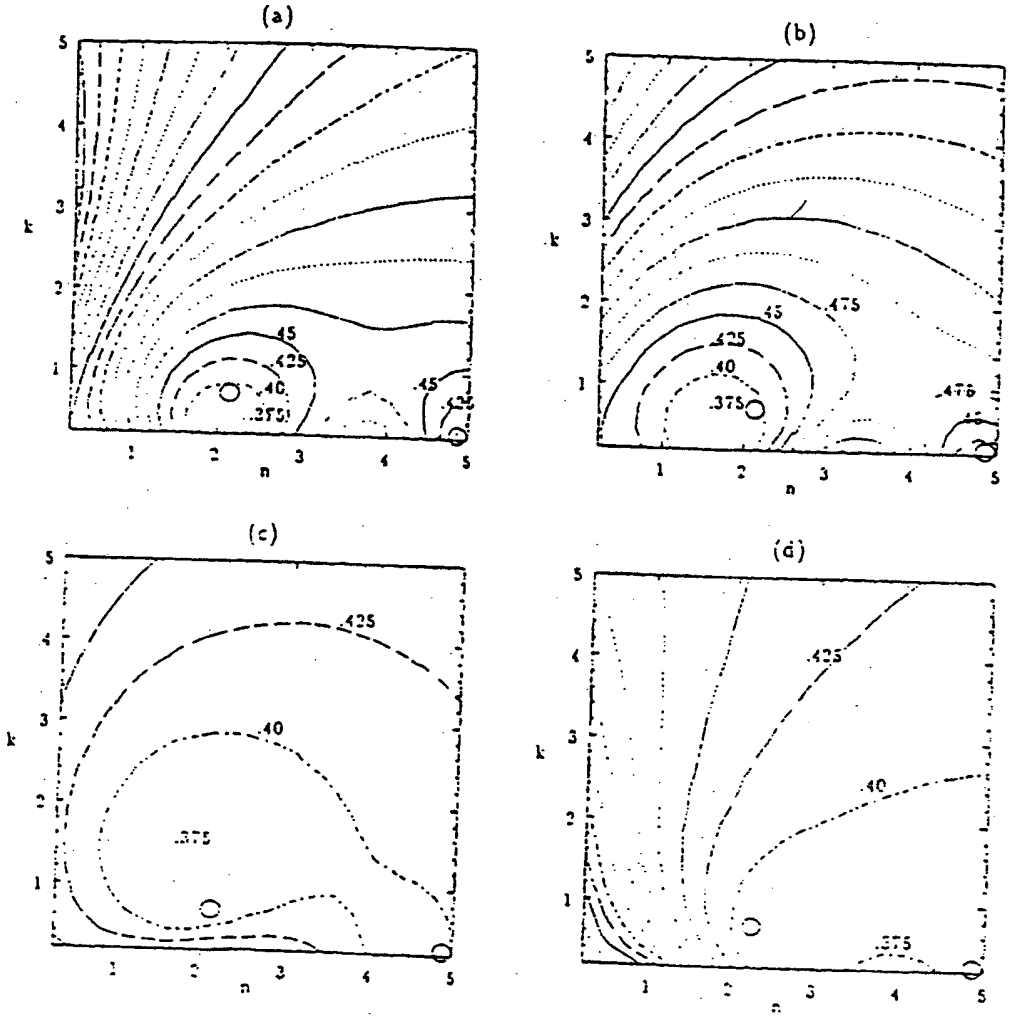

Figure 6. Calculated equi-contour line of available energy absorption. ARC thickness: 30nm, photoresis: thickness: 985nm in (a), 1000nm in (b),1020nm in (c), and 1035nm in (d).

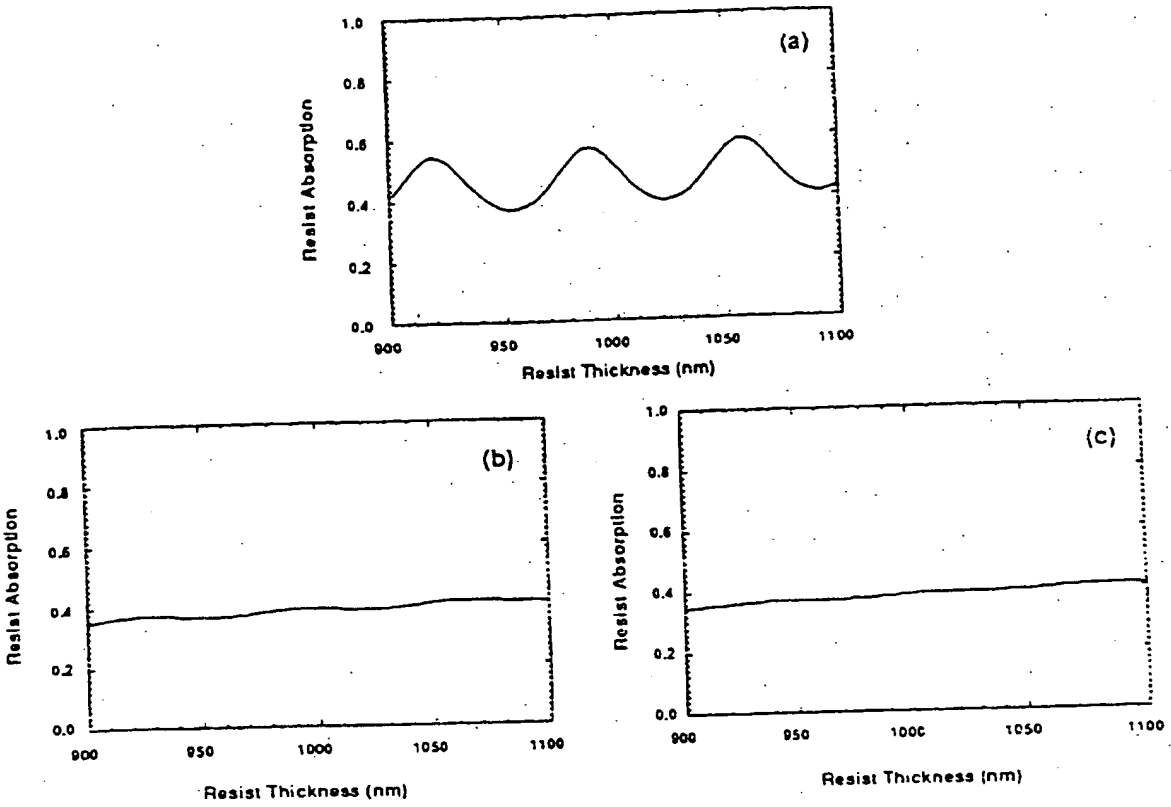

Figure 7. Resist thickness versus resist absorption for W-Si substrate with and without optimal ARC.

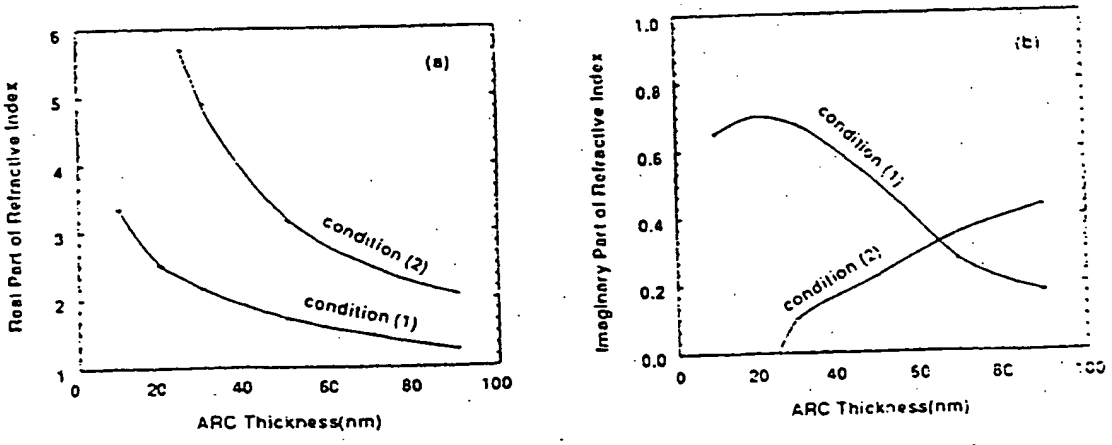

Figure 8. ARC thicknesses for W-Si substrate versus optimal refractive indices, real part(a) and imaginary part(b)

BEST AVAILABLE COPY

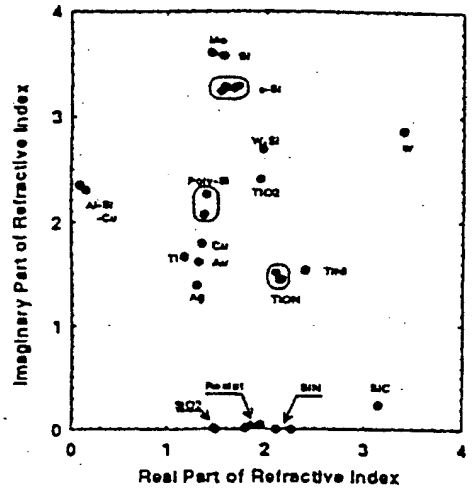

Figure 9. Refractive indices at 248nm.

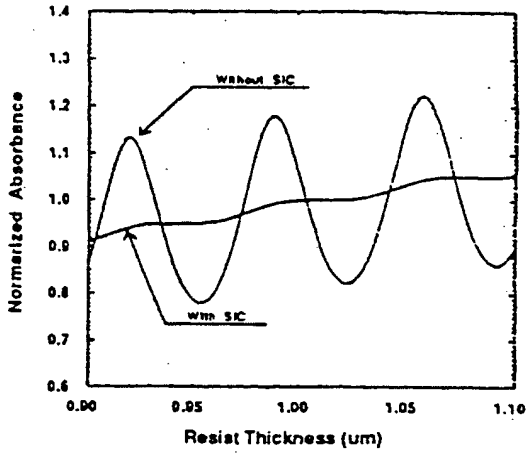

Figure 10. Thin-film interference effects, with and without SiC.

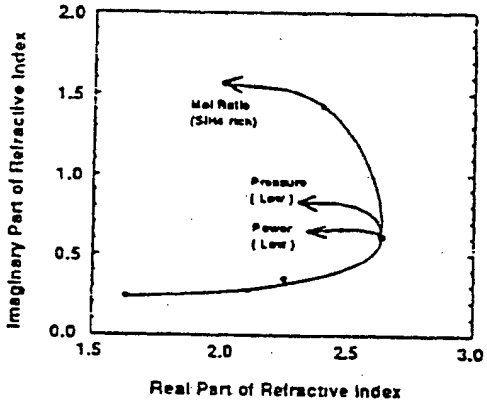

Figure 11. Optical characterization for deposition condition.

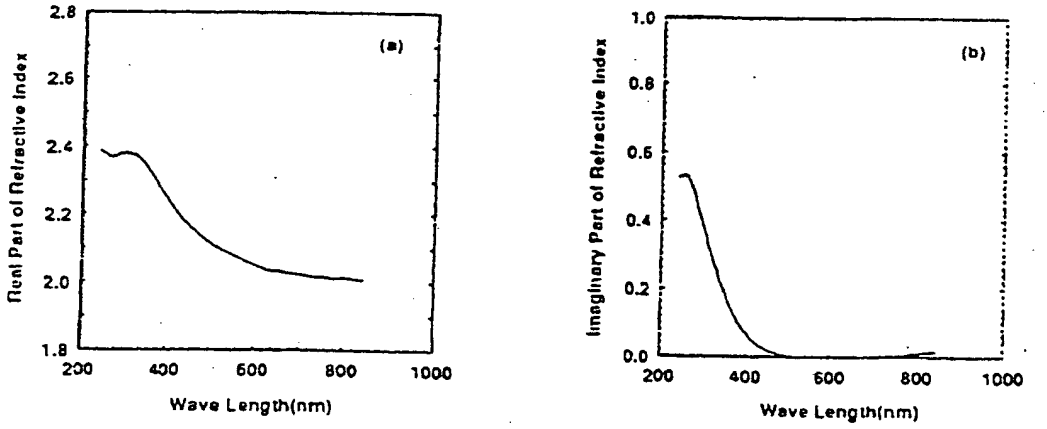

Figure 12. Wavelength versus real part(a) and imaginary part(b) of refractive index for optimized SiC film.

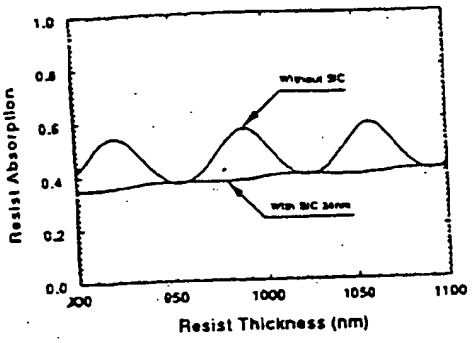

Figure13. Resist thickness versus resist absorption for with and without actual SiC film.

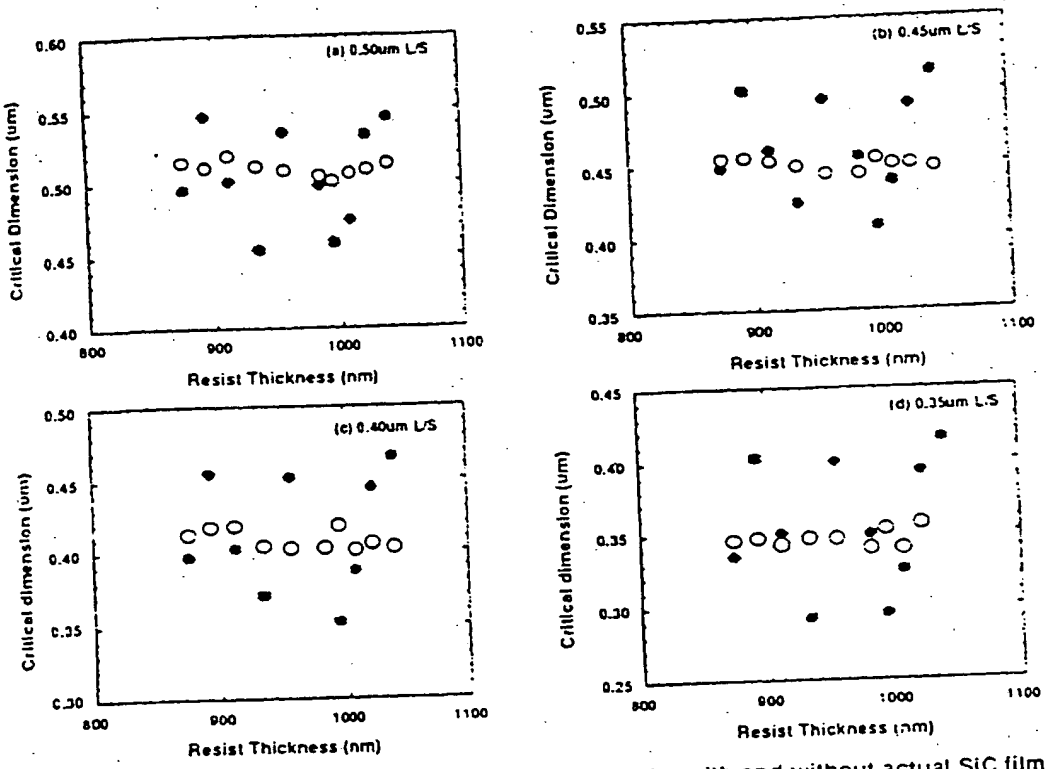

Figure14. Resist thickness versus critical dimension for with and without actual SiC film. 0.50um L/S (a), 0.45um L/S (b), 0.40um L/S (c), and 0.35um L/S (d).

Table 3. ARC performance for W-Si substrate.

geometry (K1 value)	on flat wafer		on step wafer	
	without ARC	with ARC	without ARC	with ARC
0.50um L/S (0.85)	0.092 (± 9.2 %)	0.018 (± 1.8 %)	0.088 (± 8.8 %)	0.025 (± 2.6 %)
0.45um L/S (0.76)	0.104 (± 11.6 %)	0.012 (± 1.3 %)	0.088 (± 9.8 %)	0.028 (± 3.5 %)
0.40um L/S (0.68)	0.114 (± 14.3 %)	0.017 (± 2.1 %)	0.088 (± 11.0 %)	0.035 (± 4.4 %)
0.35um L/S (0.59)	0.123 (± 17.6 %)	0.017 (± 2.4 %)	scumming (xxxxxxx)	0.032 (± 4.6 %)

(unit : um)

BEST AVAILABLE COPY

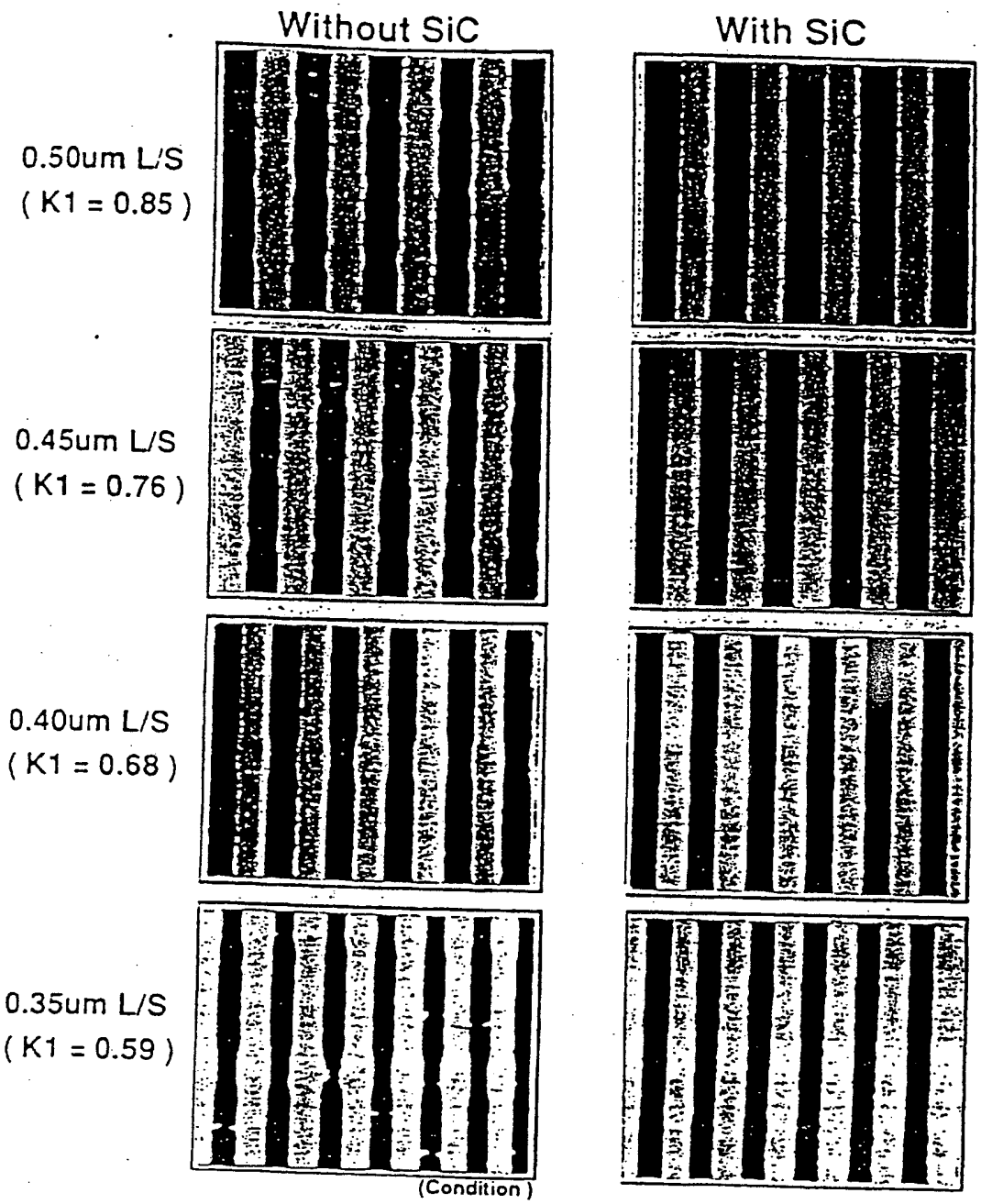

Figure 15. ARC performance for W-Si substrate